Search for Higgs boson pair production in the two bottom quarks plus two photons final state with the ATLAS detector

Corfu 2021 conference

1st September 2021

Mohamed BELFKIR

on behalf of the ATLAS Collaboration

Higgs boson pair production - HH

- **Two Higgs bosons** produced in a single pp collision
- HH cross-section is **1000**$\times$ smaller than single Higgs one
- Still **challenging**, limits on its production cross-section
- Could be enhanced by **B**eyond **S**tandard **M**odel physics:
  - **Non-resonant**: **self-coupling variation** λ
  - **Resonant**: **new particles X**

Higgs boson self-coupling

$$V \supset \frac{1}{2} m_H^2 H^2 + \lambda v H^3 + \frac{\lambda}{v} H^4$$

$$\lambda = \frac{m_H^2}{2v^2}$$

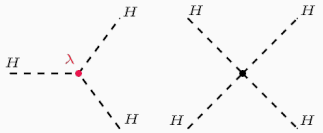

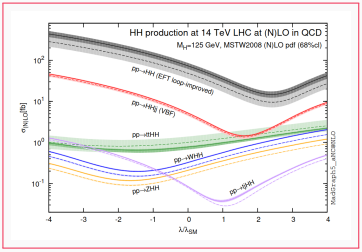

- **Higgs boson trilinear coupling**: **self-coupling**
- Controls the shape of the Higgs potential
  - $\lambda^{SM} \sim 0.13$, to be experimentally verified
- BSM modifications quantified as $\kappa_\lambda = \frac{\lambda}{\lambda^{SM}}$, can manifest as:
  - **Total** cross-section
  - **Differential** cross-section
- Measurement of $\kappa_\lambda \to \kappa_\lambda \neq 1$, presence of BSM physics

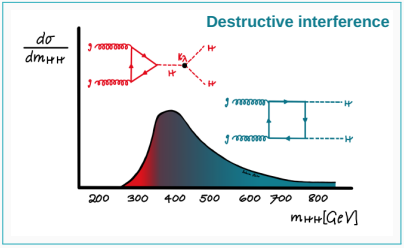

Higgs boson pair production at the LHC

- Production modes:
  - **non-resonant** at 13 TeV for $m_H = 125.09$ GeV:
    - **ggF**: $\sigma_{HH}^{ggF} = 31.02$ **fb**
    - **VBF**: $\sigma_{HH}^{VBF} = 1.72$ **fb**
  - **resonant ggF**: Spin 0 decay, $m_X \in [251, 1000]$ GeV

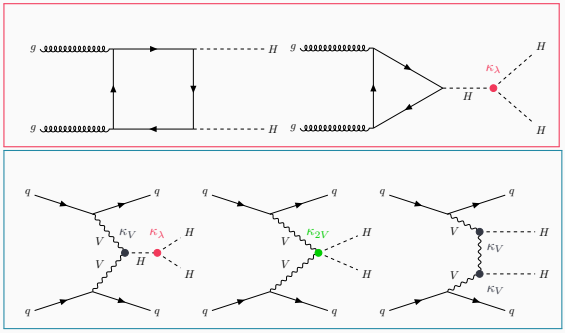

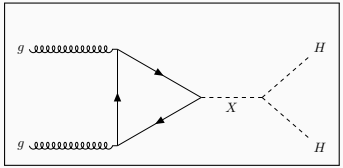

Di-Higgs boson decay modes

	bb	WW	$\tau\tau$	ZZ	$\gamma\gamma$
bb	**33%**				
WW	25%	4.6%			
$\tau\tau$	**7.4%**	2.5%	0.39%		
ZZ	3.1%	1.2%	0.34%	0.076%	
$\gamma\gamma$	**0.26%**	0.10%	0.029%	0.013%	0.0005%

ATLAS-CONF-2021-016

- **Focusing on HH$\rightarrow b\bar{b}\gamma\gamma$ (Golden channel)**
- Despite low decay rate, one of the most sensitive channels:
  - **High** H$\rightarrow b\bar{b}$ branching ratio
  - Very **clean** signature
  - **Excellent** $m_{\gamma\gamma}$ mass resolution
  - **Good signal extraction**

Di-Higgs boson decay modes

	bb	WW	$\tau\tau$	ZZ	$\gamma\gamma$
bb	**33%**				
WW	25%	4.6%			
$\tau\tau$	**7.4%**	2.5%	0.39%		
ZZ	3.1%	1.2%	0.34%	0.076%	
$\gamma\gamma$	**0.26%** ★	0.10%	0.029%	0.013%	0.0005%

ATLAS-CONF-2021-016

- **Focusing on HH$\rightarrow b\bar{b}\gamma\gamma$ (Golden channel)**
- Despite low decay rate, one of the most sensitive channels:
  - **High** H$\rightarrow b\bar{b}$ branching ratio
  - Very **clean** signature
  - **Excellent** $m_{\gamma\gamma}$ mass resolution
  - **Good signal extraction**

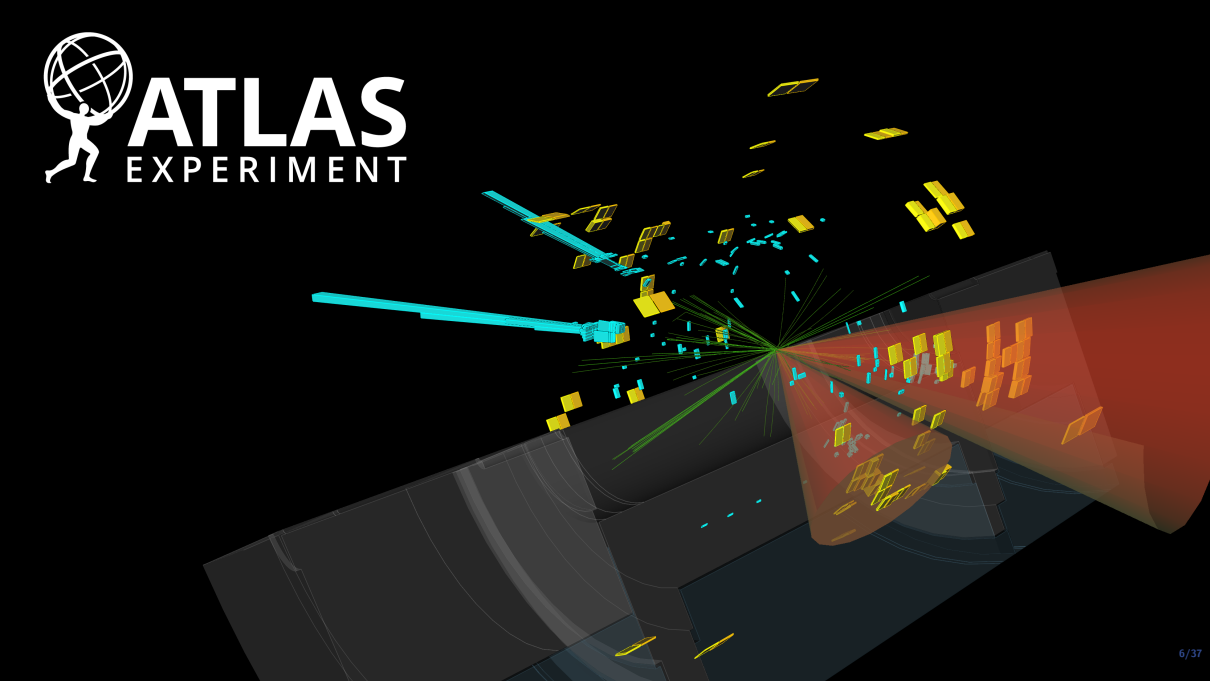
ATLAS
EXPERIMENT

Data used

- Previous search used 2015-2016 data, $\mathcal{L}_{int} = \mathbf{36.1}$ fb^{-1} **JHEP 11 (2018) 040**
- Today presentation: **search with full Run-2 data**
  - data-taking: **2015-2018**
  - $\mathcal{L}_{int} = \mathbf{139}$ **fb**$^{-1}$

	HH	HH$\rightarrow b\bar{b}\gamma\gamma$	$\sim$10% eff.
Events	4.3k	11	$\mathcal{O}(1)$

Object and event pre-selection

- **Di-photon trigger**, efficiency:
  - 83% for SM HH signal
  - 70% for resonant signal ($m_X = 300$ GeV)
- $\geq$ **2 Tight** and **isolated photons** (**H**$\rightarrow \gamma\gamma$):
  - $\frac{p_T^{\gamma}}{m_{\gamma\gamma}} > 35\%$ (25%) for leading (subleading)
  - $m_{\gamma\gamma}$, built with the two leading photons, satisfies $105 < m_{\gamma\gamma} < 160$ GeV
- **Exactly 2** b**-jet** (**H**$\rightarrow b\bar{b}$):
  - particle flow jet ($p_T > 25$ GeV & $|\eta| < 2.5$)
  - b-tagging at 77% efficiency (DL1r algorithm)
  - b-jet energy correction
- < 6 jets, reduce hadronic $t\bar{t}$H
- Zero leptons, reduce semi-leptonic $t\bar{t}$H
- Common for **resonant** and **non-resonant** analysis

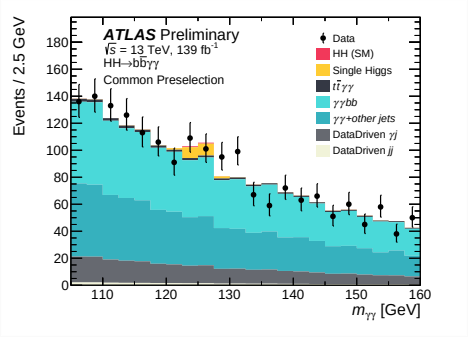

Dominant backgrounds

- **Single H**$\rightarrow \gamma\gamma$**: ggF** + $t\bar{t}H$ + **ZH**
- **Continuum** $\gamma\gamma$ + **jets**

Non-resonant categorization

- Two mass regions:
  - **High mass** $m^*_{b\bar{b}\gamma\gamma} > 350$ **GeV**
  - **Low mass** $m^*_{b\bar{b}\gamma\gamma} < 350$ **GeV**
- In each mass region, **BDT** trained to discriminating signal from backgrounds:
  - High mass: **SM HH** ($\kappa_\lambda = 1$)
  - Low mass: **BSM HH** ($\kappa_\lambda = 10$)
- Same inputs: object and event kinematic
- **4 categories**, maximum combined significance:
  - High mass: **tight** and **loose** BDT
  - Low mass: **tight** and **loose** BDT

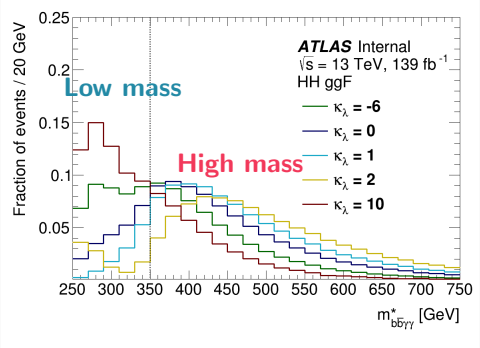

$$m^*_{b\bar{b}\gamma\gamma} = m_{b\bar{b}\gamma\gamma} - m_{b\bar{b}} - m_{\gamma\gamma} + 250 \text{ GeV}$$

Non-resonant categorization

- Two mass regions:
  - **High mass** $m^*_{b\bar{b}\gamma\gamma} > 350$ **GeV**
  - **Low mass** $m^*_{b\bar{b}\gamma\gamma} < 350$ **GeV**
- In each mass region, **BDT** trained to discriminating signal from backgrounds:
  - High mass: **SM HH** ($\kappa_\lambda = 1$)
  - Low mass: **BSM HH** ($\kappa_\lambda = 10$)
- Same inputs: object and event kinematic
- **4 categories**, maximum combined significance:
  - High mass: **tight** and **loose** BDT
  - Low mass: **tight** and **loose** BDT

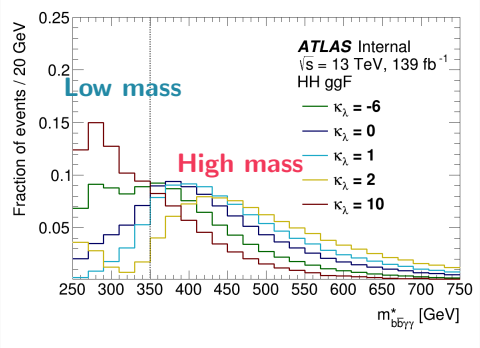

$$m^*_{b\bar{b}\gamma\gamma} = m_{b\bar{b}\gamma\gamma} - m_{b\bar{b}} - m_{\gamma\gamma} + 250 \text{ GeV}$$

Non-resonant categorization

- Two mass regions:
  - **High mass** $m^*_{b\bar{b}\gamma\gamma} > 350$ **GeV**
  - **Low mass** $m^*_{b\bar{b}\gamma\gamma} < 350$ **GeV**
- In each mass region, **BDT** trained to discriminating signal from backgrounds:
  - High mass: **SM HH** ($\kappa_\lambda = 1$)
  - Low mass: **BSM HH** ($\kappa_\lambda = 10$)
- Same inputs: object and event kinematic
- **4 categories**, maximum combined significance:
  - High mass: **tight** and **loose** BDT
  - Low mass: **tight** and **loose** BDT

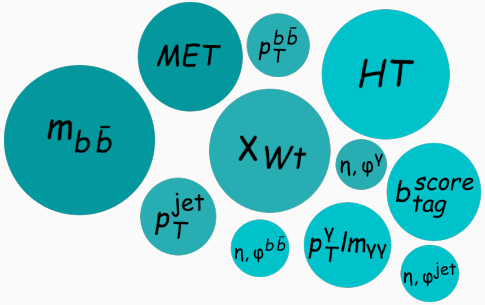

$$m^*_{b\bar{b}\gamma\gamma} = m_{b\bar{b}\gamma\gamma} - m_{b\bar{b}} - m_{\gamma\gamma} + 250 \text{ GeV}$$

Non-resonant categorization

- Two mass regions:
  - **High mass** $m^*_{b\bar{b}\gamma\gamma} > 350$ **GeV**
  - **Low mass** $m^*_{b\bar{b}\gamma\gamma} < 350$ **GeV**
- In each mass region, **BDT** trained to discriminating signal from backgrounds:
  - High mass: **SM HH** ($\kappa_\lambda = 1$)
  - Low mass: **BSM HH** ($\kappa_\lambda = 10$)
- Same inputs: object and event kinematic
- **4 categories**, maximum combined significance:
  - **High mass**: **tight** and **loose** BDT
  - **Low mass**: **tight** and **loose** BDT

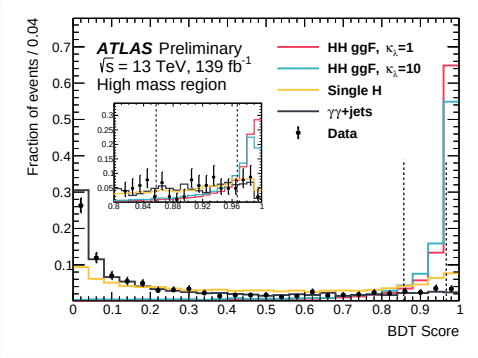

$$m^*_{b\bar{b}\gamma\gamma} = m_{b\bar{b}\gamma\gamma} - m_{b\bar{b}} - m_{\gamma\gamma} + 250 \text{ GeV}$$

Resonant categorization

- Two **BDTs** trained discriminating signal from:
  - **BDT**$_{\gamma\gamma}$: **continuum $\gamma\gamma$ +jets**
  - **BDT**$_{SingleH}$: **single Higgs**
- Inclusive training for all resonances masses
- BDTs scores **combined** in quadrature

$$\frac{1}{\sqrt{C_1^2+C_2^2}}\sqrt{C_1^2\left(\frac{\text{BDT}_{\gamma\gamma}+1}{2}\right)^2+C_2^2\left(\frac{\text{BDT}_{signleH}+1}{2}\right)^2}$$

- **1 category** maximizes significance per resonance
- $m^*_{b\bar{b}\gamma\gamma}$ cut at $\pm 2\sigma$ ($\pm 4\sigma$) for each m_X (900-1000 GeV)

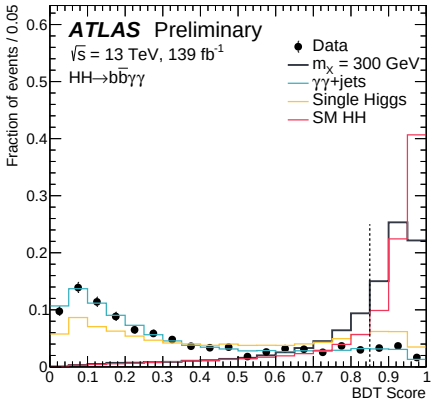

$C_2 = 1 - C_1$

Signal extraction

- **Non-resonant** & **resonant**: $m_{\gamma\gamma}$ fit
- **HH signal (ggF + VBF)**, **single Higgs** and **resonant signal**:
  - **from Monte Carlo** using Double-sided Crystal-Ball
  - **Yield parametrized as a function of κ_λ for non-resonant search**
- **Continuum $\gamma\gamma$ + jets**:
  - **fully data driven**
  - smoothly falling analytic function
  - Spurious signal test: quantify model bias $\rightarrow$ systematic uncertainty

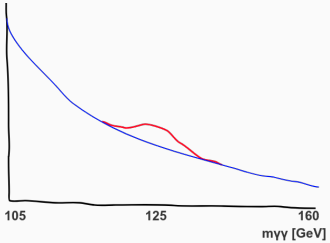

Non-resonant results

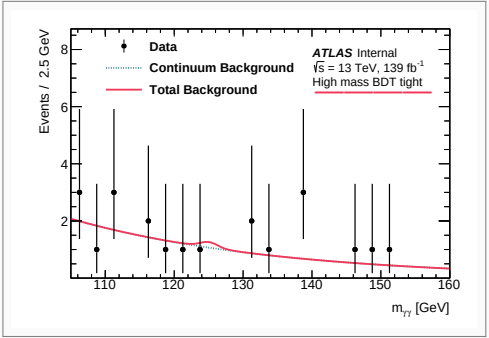

most sensitive category

- **No significant signal observed**
- $\frac{\sigma_{HH}}{\sigma_{SM}^{HH}}$ limit: **4.1** (Exp. **5.5**)
- κ_λ constrain: **[-1.5, 6.7]** (Exp. **[-2.4, 7.7]**)
- **Statistically limited**
  - Systematic effect $\sim$ **4%**
  - background modelling & photon energy scale
- **5× improvement** w.r.t 36 fb^{-1} analysis
  - Increased luminosity: 2×
  - **Analysis improvement: 3×**
    - m_{HH} categorization and MVA strategy (**80%**)
    - b-jet energy calibration (**7%**)
    - ...

Non-resonant results

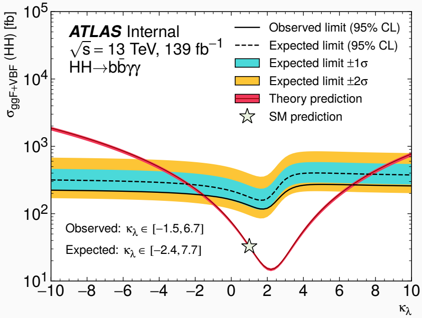

- **No significant signal observed**
- $\frac{\sigma_{HH}}{\sigma_{HH}^{SM}}$ limit: **4.1** (Exp. **5.5**)
- κ_λ constrain: **[-1.5, 6.7]** (Exp. **[-2.4, 7.7]**)
- Statistically limited
  - Systematic effect ∼ **4%**
  - Background modelling & photon energy scale
- 5× **improvement** w.r.t 36 fb^{-1} analysis
  - Increased luminosity: 2×
  - **Analysis improvement: 3×**
    - m_{HH} categorization and MVA strategy (**80%**)
    - *b*-jet energy calibration (**7%**)
    - ...

World's best limit

Non-resonant results

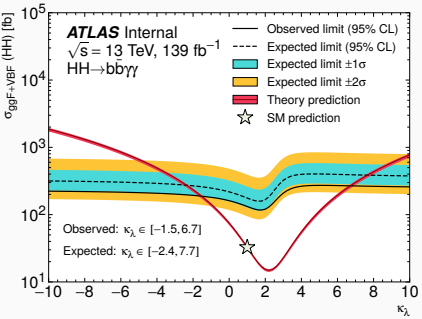

- **No significant signal observed**
- $\frac{\sigma_{HH}}{\sigma_{HH}^{SM}}$ limit: **4.1** (Exp. **5.5**)
- κ_λ constrain: **[-1.5, 6.7]** (Exp. **[-2.4, 7.7]**)
- **Statistically limited**
  - Systematic effect $\sim$ **4%**
  - background modelling & photon energy scale
- **5× improvement** w.r.t 36 fb^{-1} analysis
  - Increased luminosity: 2×
  - **Analysis improvement: 3×**
    - m_{HH} categorization and MVA strategy (**80%**)
    - b-jet energy calibration (**7%**)
    - ...

Non-resonant results

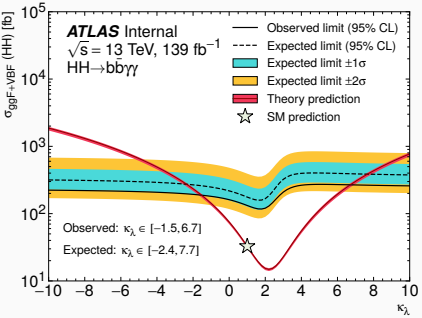

- **No significant signal observed**
- $\frac{\sigma_{HH}}{\sigma_{HH}^{SM}}$ limit: **4.1** (Exp. **5.5**)
- κ_λ constrain: **[-1.5, 6.7]** (Exp. **[-2.4, 7.7]**)
- **Statistically limited**
  - Systematic effect $\sim$ **4%**
  - background modelling & photon energy scale
- **5× improvement** w.r.t 36 fb^{-1} analysis
  - Increased luminosity: 2×
  - **Analysis improvement: 3×**
    - m_{HH} categorization and MVA strategy (**80%**)
    - b-jet energy calibration (**7%**)
    - ...

Resonant results

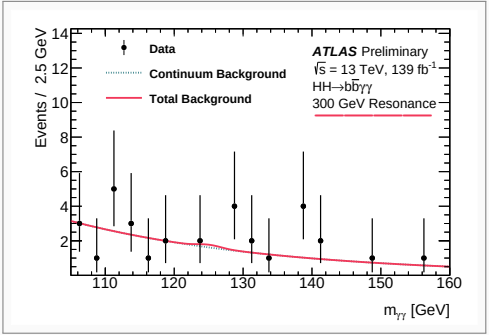

- **No significant excess is observed**
- $\sigma_{X \to HH}$ limit: **610-47 fb** (Exp. **360-43 fb**)
- **Statistically limited**
  - Systematic effect **up to 10%**
  - background modelling & photon energy scale
- **30% improvement** from BDT w.r.t 36 fb^{-1} on top luminosity increase

Resonant results

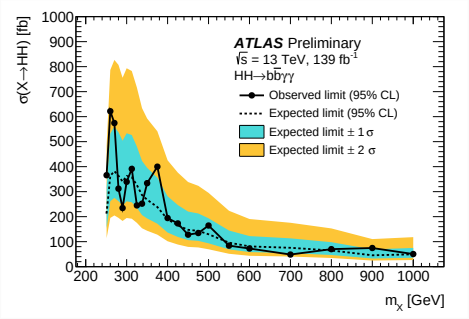

- **No significant excess is observed**
- $\sigma_{X\to HH}$ limit: **610-47 fb** (Exp. **360-43 fb**)
- **Statistically limited**
  - Systematic effect **up to 10%**
  - background modelling & photon energy scale
- **30% improvement** from BDT w.r.t 36 fb^{-1} on top luminosity increase

Resonant results

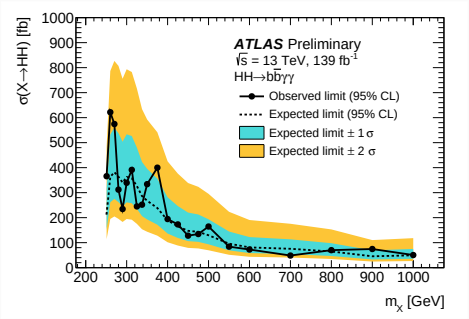

- **No significant excess is observed**
- $\sigma_{X \to HH}$ limit: **610-47 fb** (Exp. **360-43 fb**)
- **Statistically limited**
  - Systematic effect **up to 10%**
  - background modelling & photon energy scale
- **30% improvement** from BDT w.r.t 36 fb^{-1} on top luminosity increase

Resonant results

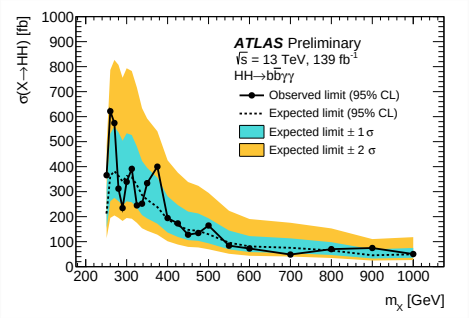

- **No significant excess is observed**
- $\sigma_{X \to HH}$ limit: **610-47 fb** (Exp. **360-43 fb**)
- **Statistically limited**
  - Systematic effect **up to 10%**
  - background modelling & photon energy scale
- **30% improvement** from BDT w.r.t 36 fb^{-1} on top luminosity increase

Summary

- **Non-resonant** and **resonant** HH→ $b\bar{b}\gamma\gamma$ searches using the full Run-2 data (139 fb^{-1})
- Other channels are published:
  - **Resonant HH→** $b\bar{b}b\bar{b}$: ATLAS-CONF-2021-035
  - **Resonant & Non-resonant HH→** $b\bar{b}\tau\tau$: ATLAS-CONF-2021-030
- Resonant & Non-resonant comparisons: ATL-PHYS-PUB-2021-031

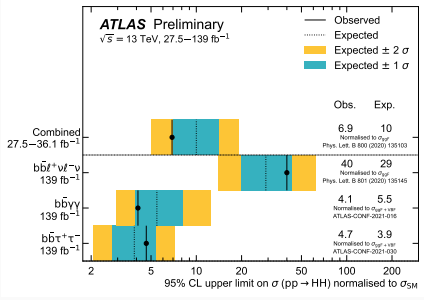

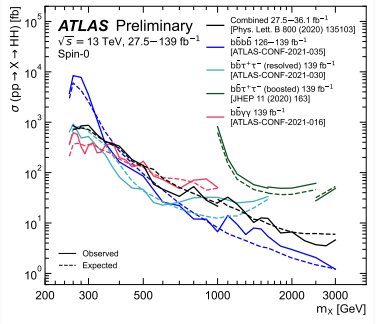

- Great improvement in Run-2, **ready to Run-3**

Thank you for your attention

BACKUP

Large Hadron Collider

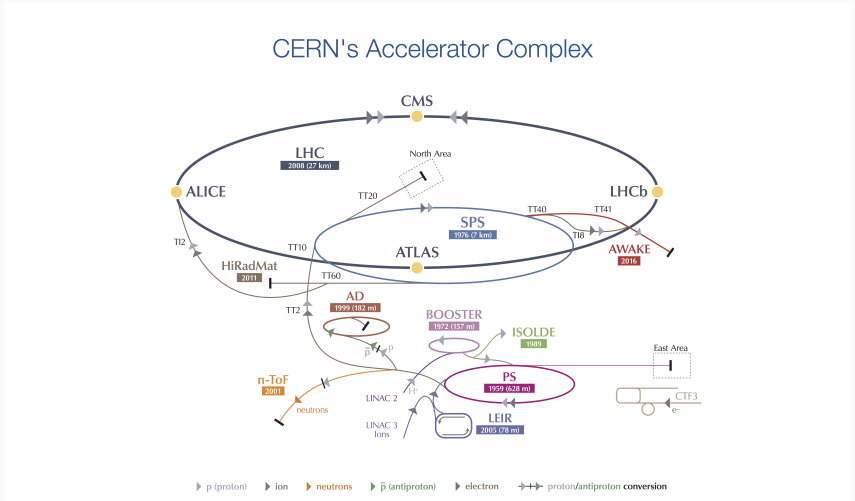

ATLAS detector

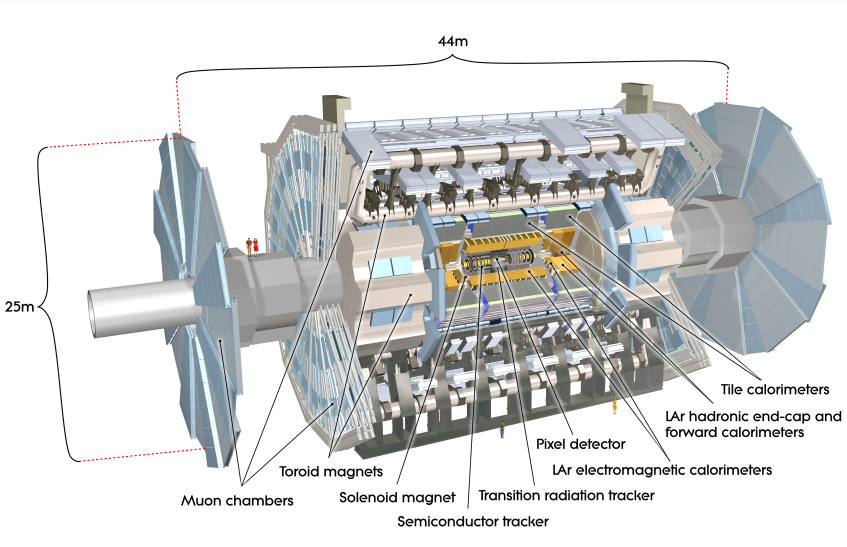

Di-Higgs - production modes

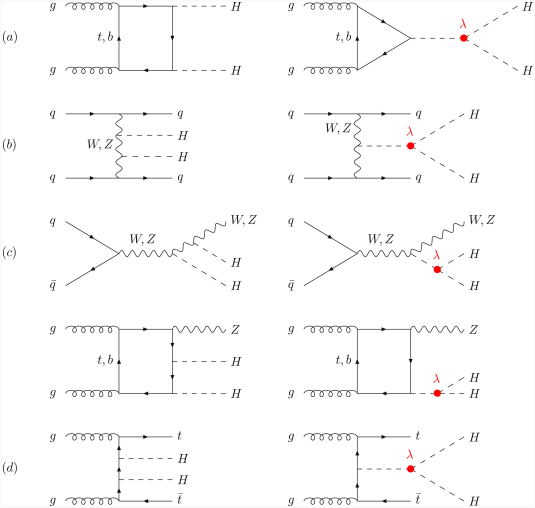

Di-Higgs - cross-section

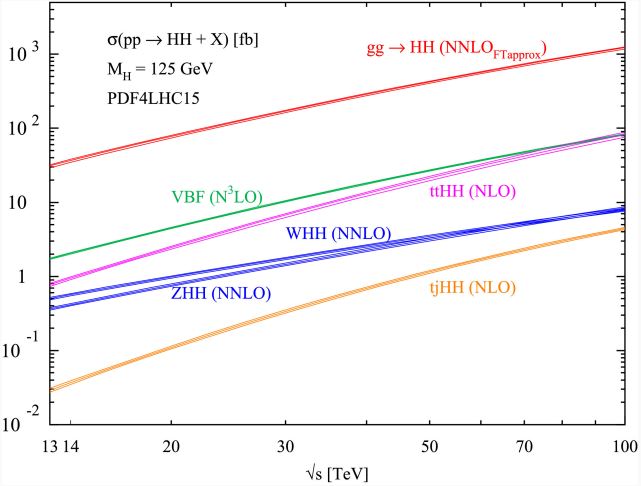

Data and Monte Carlo samples

- **ggF HH signal** ($\kappa_\lambda = 1, 10$) at NLO with **Powheg-Box** v2 PDF4LHC15 + **Pythia 8**
- **VBF HH signal** ($\kappa_\lambda = 0, 1, 2, 10$) at LO with **MadGraph5_aMC@NLO** v2.6.0 NNPDF3.0nlo + **Pythia 8**
- **resonant spin-0** X→HH via ggF at LO with **MadGraph5_aMC@NLO** v2.6.1 NNPDF2.3lo + **Herwig** v7.1.3. $m_X \in [251, 1000]$ GeV and $\Lambda_X = 10$ MeV

Process	Generator	PDF set	Showering	Tune
ggF	NNLOPS	PDFLHC	Pythia 8.2	AZNLO
VBF	Powheg Box v2	PDFLHC	Pythia 8.2	AZNLO
WH	Powheg Box v2	PDFLHC	Pythia 8.2	AZNLO
$qq \to ZH$	Powheg Box v2	PDFLHC	Pythia 8.2	AZNLO
$gg \to ZH$	Powheg Box v2	PDFLHC	Pythia 8.2	AZNLO
$t\bar{t}H$	Powheg Box v2	NNPDF3.0nlo	Pythia 8.2	A14
bbH	Powheg Box v2	NNPDF3.0nlo	Pythia 8.2	A14
$tHqj$	MadGraph5_aMC@NLO	NNPDF3.0nlo	Pythia 8.2	A14
tHW	MadGraph5_aMC@NLO	NNPDF3.0nlo	Pythia 8.2	A14
$\gamma\gamma$+jets	Sherpa v2.2.4	NNPDF3.0nnlo	Sherpa v2.2.4	–
$t\bar{t}\gamma\gamma$	MadGraph5_aMC@NLO	NNPDF2.3lo	Pythia 8.2	–

$m^*_{b\bar{b}\gamma\gamma}$ variable

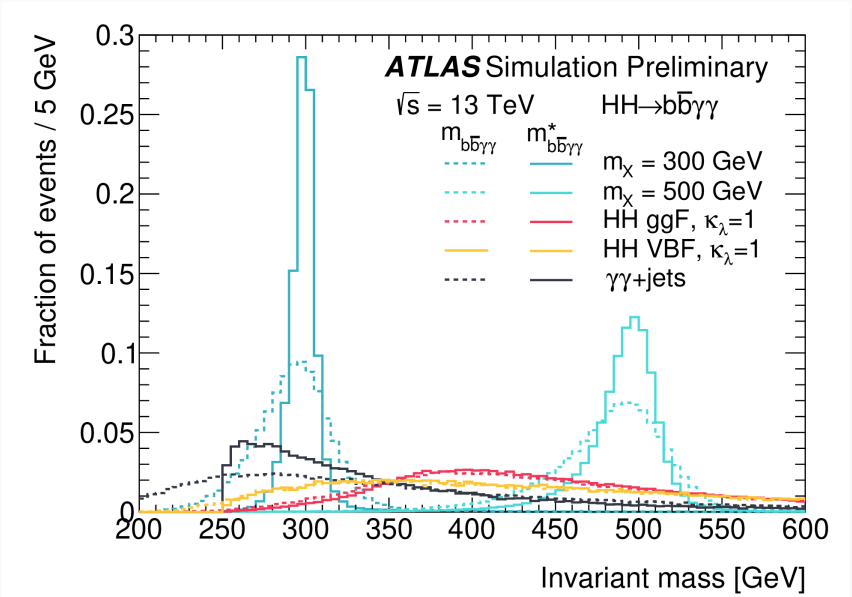

$m^*_{b\bar{b}\gamma\gamma}$ for ggF vs VBF HH

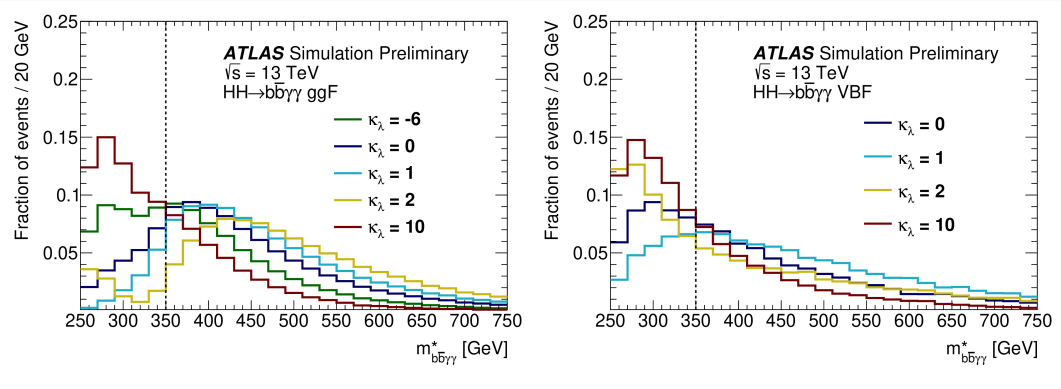

non-resonant BDT variables

Variable	Definition
Photon-related kinematic variables	
$p_T/m_{\gamma\gamma}$	Transverse momentum of the two photons scaled by their invariant mass $m_{\gamma\gamma}$
η and ϕ	Pseudo-rapidity and azimuthal angle of the leading and sub-leading photon
Jet-related kinematic variables	
b-tag status	Highest fixed b-tag working point that the jet passes
p_T, η and ϕ	Transverse momentum, pseudo-rapidity and azimuthal angle of the two jets with the highest b-tagging score
$p_T^{b\bar{b}}$, $\eta_{b\bar{b}}$ and $\phi_{b\bar{b}}$	Transverse momentum, pseudo-rapidity and azimuthal angle of b-tagged jets system
$m_{b\bar{b}}$	Invariant mass built with the two jets with the highest b-tagging score
H_T	Scalar sum of the p_T of the jets in the event
Single topness	For the definition, see Eq. (**??**)
Missing transverse momentum-related variables	
E_T^{miss} and ϕ^{miss}	Missing transverse momentum and its azimuthal angle

$$\chi_{Wt} = \min \sqrt{\left(\frac{m_{j_1 j_2} - m_W}{m_W}\right)^2 + \left(\frac{m_{j_1 j_2 j_3} - m_t}{m_t}\right)^2}$$

non-resonant BDT scores

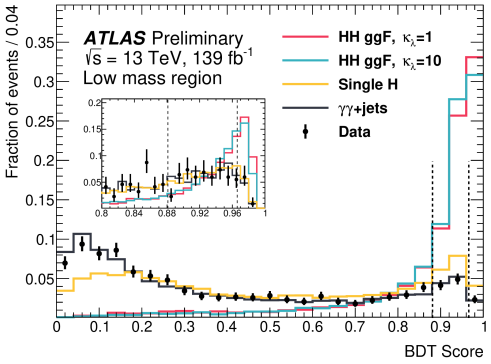

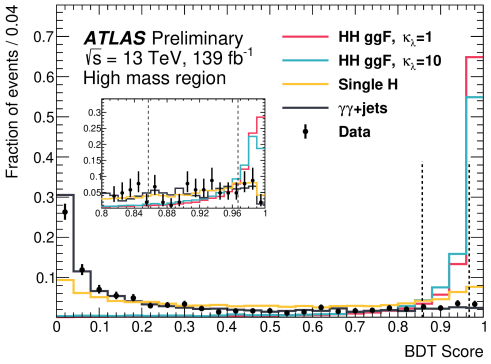

Category	Selection criteria
High mass BDT tight	$m^*_{bb\gamma\gamma} \geq 350$ GeV, BDT score $\in [0.967, 1]$
High mass BDT loose	$m^*_{bb\gamma\gamma} \geq 350$ GeV, BDT score $\in [0.857, 0.967]$
Low mass BDT tight	$m^*_{bb\gamma\gamma} < 350$ GeV, BDT score $\in [0.966, 1]$
Low mass BDT loose	$m^*_{bb\gamma\gamma} < 350$ GeV, BDT score $\in [0.881, 0.966]$

resonant BDT variables

Variable	Definition
Photon-related kinematic variables	
$p_{\mathrm{T}}^{\gamma\gamma}$, $y^{\gamma\gamma}$	Transverse momentum and rapidity of the di-photon system
$\Delta\phi_{\gamma\gamma}$ and $\Delta R_{\gamma\gamma}$	Azimuthal angular distance and ΔR between the two photons
Jet-related kinematic variables	
$m_{b\bar{b}}$, $p_{\mathrm{T}}^{b\bar{b}}$ and $y_{b\bar{b}}$	Invariant mass, transverse momentum and rapidity of the b-tagged jets system
$\Delta\phi_{b\bar{b}}$ and $\Delta R_{b\bar{b}}$	Azimuthal angular distance and ΔR between the two b-tagged jets
N_{jets} and $N_{b-\mathrm{jets}}$	Number of jets and number of b-tagged jets
H_{T}	Scalar sum of the p_{T} of the jets in the event
Photons and jets-related kinematic variables	
$m_{b\bar{b}\gamma\gamma}$	Invariant mass built with the di-photon and b-tagged jets system
$\Delta y_{\gamma\gamma,b\bar{b}}$, $\Delta\phi_{\gamma\gamma,b\bar{b}}$ and $\Delta R_{\gamma\gamma,b\bar{b}}$	Distance in rapidity, azimuthal angle and ΔR between the di-photon and the b-tagged jets system

resonant BDT scores

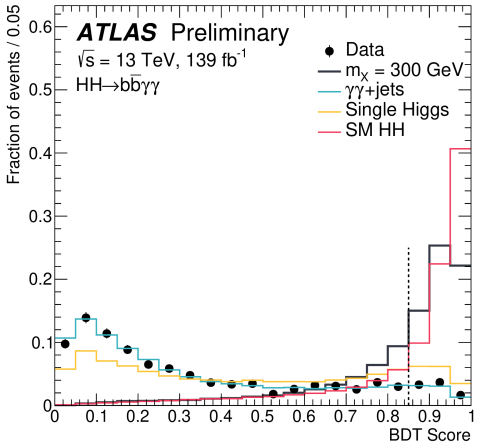

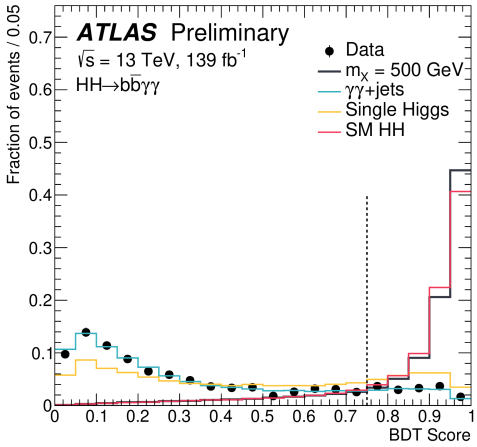

non-resonant data/MC

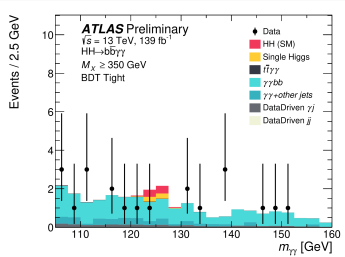

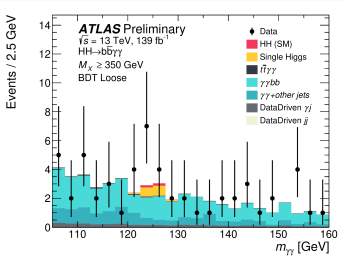

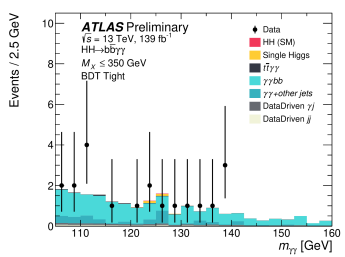

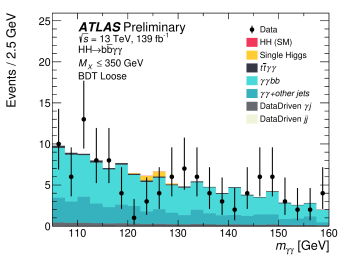

background-only fit : non-resonant

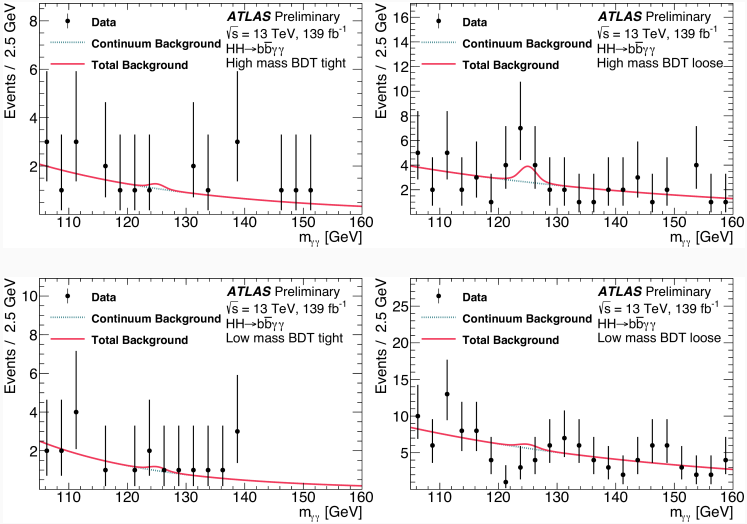

resonant data/MC

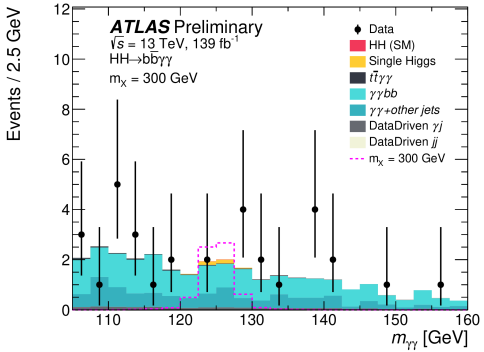

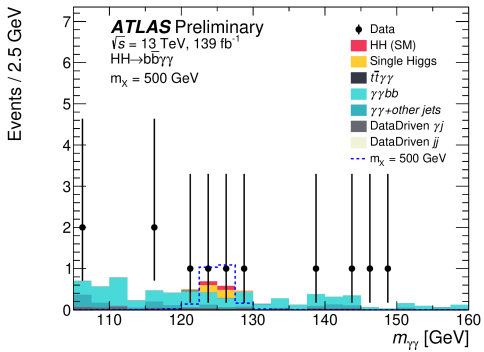

background-only fit : resonant

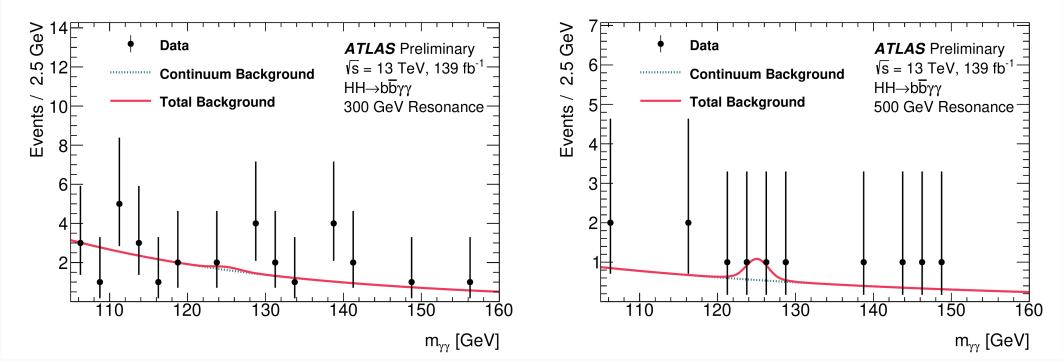

Expected and observed numbers of events of the non-resonant HH search

	High mass BDT tight	High mass BDT loose	Low mass BDT tight	Low mass BDT loose
Continuum background	4.9 ± 1.1	9.5 ± 1.5	3.7 ± 1.0	24.9 ± 2.5
Single Higgs boson background	0.670 ± 0.032	1.57 ± 0.04	0.220 ± 0.016	1.39 ± 0.04
ggF	0.261 ± 0.028	0.44 ± 0.04	0.063 ± 0.014	0.274 ± 0.030
$t\bar{t}H$	0.1929 ± 0.0045	0.491 ± 0.007	0.1074 ± 0.0033	0.742 ± 0.009
ZH	0.142 ± 0.005	0.486 ± 0.010	0.04019 ± 0.0027	0.269 ± 0.007
Rest	0.074 ± 0.012	0.155 ± 0.020	0.008 ± 0.006	0.109 ± 0.016
SM HH signal	0.8753 ± 0.0032	0.3680 ± 0.0020	$(49.4 \pm 0.7) \cdot 10^{-3}$	$(78.7 \pm 0.9) \cdot 10^{-3}$
ggF	0.8626 ± 0.0032	0.3518 ± 0.0020	$(46.1 \pm 0.7) \cdot 10^{-3}$	$(71.8 \pm 0.9) \cdot 10^{-3}$
VBF	0.01266 ± 0.00016	0.01618 ± 0.00018	$(3.22 \pm 0.08) \cdot 10^{-3}$	$(6.923 \pm 0.011) \cdot 10^{-3}$
Alternative $HH(\kappa_\lambda = 10)$ signal	6.36 ± 0.05	3.691 ± 0.038	4.65 ± 0.04	8.64 ± 0.06
Data	2	17	5	14

Expected and observed numbers of events of the resonant HH search

	$m_X = 300$ GeV	$m_X = 500$ GeV
Continuum background	5.6 ± 2.4	3.5 ± 2.0
Single Higgs boson background	0.339 ± 0.009	0.398 ± 0.010
SM HH background	$(20.6 \pm 0.5) \cdot 10^{-3}$	0.1932 ± 0.0015
$X \to HH$ signal	5.771 ± 0.031	5.950 ± 0.026
Data	6	4

Syetamtic impact

		Relative impact of the systematic uncertainties in %	
Source	Type	Non-resonant analysis HH	Resonant analysis m_X = 300 GeV
Experimental			
Photon energy scale	Norm. + Shape	5.2	2.7
Photon energy resolution	Norm. + Shape	1.8	1.6
Flavor tagging	Normalization	0.5	< 0.5
Theoretical			
Heavy flavor content	Normalization	1.5	< 0.5
Higgs boson mass	Norm. + Shape	1.8	< 0.5
PDF+α_s	Normalization	0.7	< 0.5
Spurious signal	Normalization	5.5	5.4

HH$\to b\bar{b}\gamma\gamma$ 36 fb^{-1} results

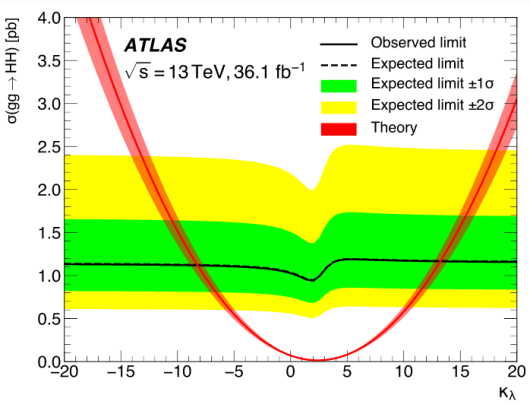

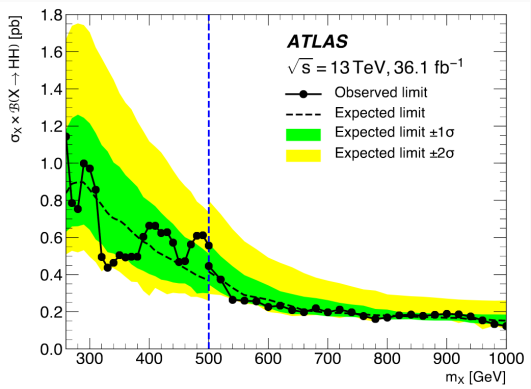

CMS full Run-2 results

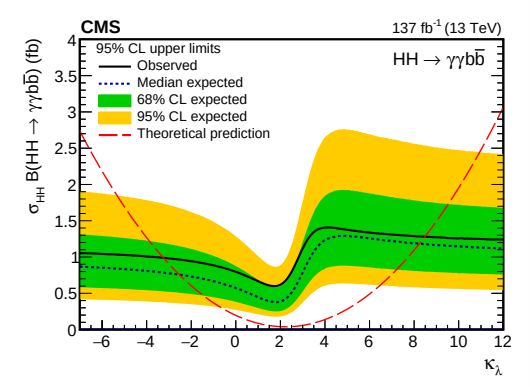

	Expected	Observed
CMS $\frac{\sigma_{HH}}{\sigma_{HH}^{SM}}$ limit	**5.2**	7.7
CMS κ_λ interval	**[-2.5, 8.2]**	[-3.3, 8.5]
ATLAS $\frac{\sigma_{HH}}{\sigma_{HH}^{SM}}$ limit	**5.5**	4.1
ATLAS κ_λ interval	**[-2.4, 7.7]**	[-1.5, 6.7]

Early Run-2 combination